

The Waterbed Effect on Quasiperiodic Disturbance Observer: Avoidance of Sensitivity Tradeoff with Time Delays^{*}

Hisayoshi Muramatsu^{*}

^{*} *Mechanical Engineering Program, Hiroshima University, Higashihiroshima, Hiroshima, 739-8527, Japan (e-mail: muramatsu@hiroshima-u.ac.jp).*

Abstract: In linear time-invariant systems, the sensitivity function to disturbances is designed under a sensitivity tradeoff known as the waterbed effect. To compensate for a quasiperiodic disturbance, a quasiperiodic disturbance observer using time delays was proposed. Its sensitivity function avoids the sensitivity tradeoff, achieving wideband harmonic suppression without amplifying aperiodic disturbances or shifting harmonic suppression frequencies. However, its open-loop transfer function is not rational and does not satisfy the assumptions of existing Bode sensitivity integrals due to its time delays. This paper provides Bode-like sensitivity integrals for the quasiperiodic disturbance observer in both continuous-time and discrete-time representations and clarifies the avoided sensitivity tradeoff with time delays.

Keywords: Disturbance observer, time delays, harmonics, repetitive control, iterative learning control, sensitivity function, waterbed effect, Bode sensitivity integral

1. INTRODUCTION

One of the fundamental issues in automatic control is disturbance compensation. In practical systems, disturbances always exist and impair the precision of automatic control. For linear time-invariant systems, we design a sensitivity function $S(s) := 1/(1 + \Gamma(s))$ based on an open-loop transfer function $\Gamma(s)$, while tradeoffs restrict the design. One tradeoff lies between the sensitivity function $S(s) := 1/(1 + \Gamma(s))$ and complementary sensitivity function $T(s) := \Gamma(s)/(1 + \Gamma(s))$, which are restricted by the unit sum $S(s) + T(s) = 1$. The sensitivity and complementary sensitivity functions represent disturbance-suppression performance and robust stability against modeling errors, respectively. It is necessary to reduce their gains appropriately to improve performance under the unit-sum tradeoff. For the sensitivity function, there exists another tradeoff in the sensitivity integral given by Bode (1945). This Bode sensitivity integral (Freudenberg and Looze (1985); Ding et al. (2022); Nagarsheth and Sharma (2021)) states that a stable sensitivity function satisfies

$$\int_0^\infty \ln |S(j\omega)| d\omega = \pi \sum_i \operatorname{Re}[q_i] - \frac{\pi}{2} \lim_{s \rightarrow \infty} s\Gamma(s), \quad (1)$$

where q_i are the unstable right-half-plane poles of a proper rational function $\Gamma(s)$. Also, Wu and Jonckheere (1992); Sung and Hara (1988); Mohtadi (1990); Emami-Naeini and de Roover (2019) provide the Bode sensitivity integral for discrete-time control. Based on a rational open-

loop transfer function $\tilde{\Gamma}(z)$, the stable sensitivity function $\tilde{S}(z) := 1/(1 + \tilde{\Gamma}(z))$ satisfies

$$\int_0^{2\pi} \ln |\tilde{S}(e^{j\omega})| d\omega = 2\pi \sum_i \ln |\tilde{q}_i| - 2\pi \ln \left| \lim_{z \rightarrow \infty} \tilde{\Gamma}(z) + 1 \right|, \quad (2)$$

where \tilde{q}_i are unstable poles outside the closed-unit disk of a proper rational function $\tilde{\Gamma}(z)$. The Bode sensitivity integral is called the waterbed effect (Skogestad and Postlethwaite (2005); Costa-Castelló and Dormido (2015)), as the gain increases at some frequencies while decreasing at other frequencies. However, these Bode sensitivity integrals are applicable only to proper rational open-loop transfer functions.

Periodic disturbances often occur in automatic mechanical and electrical systems. To compensate for harmonics of a periodic disturbance, time delays are essential. Repetitive control (Hara et al. (1988)), iterative learning control (Wang et al. (2009); Bristow et al. (2006)), and periodic disturbance observers (Muramatsu and Katsura (2018)) have been proposed using time delays for an internal model of a periodic disturbance. However, in designing the sensitivity function with time delays, a waterbed-effect-like tradeoff exists between the wideband harmonic suppression, amplification of aperiodic disturbances, and deviation of harmonic suppression frequencies (Pipeleers et al. (2008); Chen and Tomizuka (2014); Nie et al. (2021); Tanaka and Muramatsu (2023); Yang et al. (2023); Lai et al. (2021); Li et al. (2023)). To overcome the tradeoff, Muramatsu (2025) proposed a quasiperiodic disturbance observer (QDOB) using time delays, which achieved wideband harmonic suppression, non-amplification of aperiodic disturbances, and non-deviation of harmonic suppression

^{*} This work was supported by JSPS KAKENHI Grant Number JP25K17560.

This paper has been published in *IFAC Journal of Systems and Control*, vol. 35, p. 100392, Mar. 2026.
See <https://doi.org/10.1016/j.ifacsc.2026.100392>

frequencies, simultaneously. From the perspective of the Bode sensitivity integral, this paper examines the waterbed effect on the QDOB in both continuous-time and discrete-time representations.

The Bode sensitivity integral for disturbance observers based on rational transfer functions has been studied by [Sariyildiz and Ohnishi \(2013a,b\)](#). However, the results cannot be applied to the QDOB by [Muramatsu \(2025\)](#), whose open-loop transfer function is

$$\Gamma(s) = \frac{\omega_c L}{2} \frac{1 + \Phi(s)}{1 - \Phi(s)} \frac{\omega_b}{s + \omega_b}, \quad (3)$$

where $\omega_b, \omega_c, L \in \mathbb{R}_{>0}$. The function $\Phi(s)$ is a linear-phase low-pass filter that can be expressed as

$$\Phi(s) = e^{-\kappa Ts} \prod_{i=1}^l \sum_{n=-N}^N \frac{\alpha_i(n)}{\gamma_i} e^{(n-N)T\bar{U}_i s}, \quad (4)$$

where $\kappa := \bar{L} - N \sum_{i=1}^l \bar{U}_i \geq 1$, $\bar{U}_i := \text{round}(U_i/T)$, and $\bar{L} := \text{round}(L/T)$. The open-loop transfer function has an infinite number of zeros by $1 + \Phi(s)$ and an infinite number of poles by $1 - \Phi(s)$ on the imaginary axis. Consequently, the open-loop transfer function $\Gamma(s)$ is not rational and is a meromorphic function with time delays.

Several studies have extended the class of open-loop transfer functions applicable to the Bode sensitivity integral. [Freudenberg and Looze \(1987\)](#) investigated the Bode sensitivity integral with an open-loop transfer function $\Gamma_0(s)e^{-\tau s}$ combining a rational function $\Gamma_0(s)$ and time delay $e^{-\tau s}$. In the discrete-time domain, the integral with iterative learning control was examined by [Songchon and Longman \(2000\)](#). Besides, [Chang et al. \(2023\)](#) considered fractional-order proportional-integral-derivative control, while this paper does not consider such irrational fractional-order open-loop transfer functions. Furthermore, [Gomez and Goodwin \(1998\)](#) obtained the Bode sensitivity integral for meromorphic functions with time delays; however, it cannot address an infinite number of zeros of the sensitivity function on the imaginary axis, such as the QDOB.

The main results of this paper are the theorems of Bode-like sensitivity integrals for the QDOB in both continuous-time and discrete-time representations. Through the theorems and numerical integration results, this paper demonstrates how the QDOB avoids the waterbed effect.

2. PRELIMINARIES

This section presents the QDOB proposed by [Muramatsu \(2025\)](#) as preliminaries. Suppose the single-input-single-output plant

$$\mathcal{L}[y(t)] = P(s)\mathcal{L}[u(t) + v(t)], \quad (5)$$

where

$$P(s) := (1 + \Delta(s))P_n(s) \quad (6a)$$

$$P_n(s) := \frac{b_n s^n + b_{n-1} s^{n-1} + \dots + b_1 s + b_0}{s^m + a_{m-1} s^{m-1} + \dots + a_1 s + a_0} \quad (6b)$$

$$\Delta(s) := \frac{\beta_g s^g + \beta_{g-1} s^{g-1} + \dots + \beta_1 s + \beta_0}{s^h + \alpha_{h-1} s^{h-1} + \dots + \alpha_1 s + \alpha_0} e^{-\gamma s} \quad (6c)$$

with $n, m, g, h \in \mathbb{Z}_{\geq 0}$, $n < m$, and $\gamma \in \mathbb{R}_{\geq 0}$. The symbols $t \in \mathbb{R}$, $u(t) \in \mathbb{R}$, $v(t) \in \mathbb{R}$, $y(t) \in \mathbb{R}$, $P(s) \in \mathbb{C}$, $P_n(s) \in \mathbb{C}$,

$\Delta(s) \in \mathbb{C}$, and \mathcal{L} denote the time, input, exogenous signal, output, plant, nominal plant, stable modeling error, and Laplace transform operator, respectively. Assume that the strictly proper transfer function $P_n(s)$ has no zeros or poles in the closed right-half plane. For the plant, the disturbance $d(t)$ including the exogenous signal and effects of the modeling error is defined as

$$\mathcal{L}[d(t)] := \mathcal{L}[v(t)] + \Delta(s)\mathcal{L}[u(t) + v(t)], \quad (7)$$

and the plant is rewritten as

$$\mathcal{L}[y(t)] = P_n(s)\mathcal{L}[u(t) + d(t)]. \quad (8)$$

Using the lifting transform \mathcal{G} and the discrete-time Fourier transform \mathcal{F} :

$$\mathcal{G}[d]_{L,\tau}(c) := d(cL + \tau), \quad L \in \mathbb{R}_{>0}, \tau \in [0, L), c \in \mathbb{Z} \quad (9a)$$

$$\mathcal{F}[D](\Omega) := \sum_{c=-\infty}^{\infty} D(c)e^{-j\Omega c}, \quad (9b)$$

where $\Omega \in [0, 2\pi)$ [rad/sample] denotes the normalized angular frequency. Then, the definition of a quasiperiodic disturbance given in [Muramatsu \(2025\)](#) can be stated as Definition 2.1.

Definition 2.1. A disturbance $d \in \mathcal{D}_L$ is called quasiperiodic with respect to a period $L \in \mathbb{R}_{>0}$ and separation frequency $\rho \in [0, \pi/L)$ if $d \in \mathcal{P}_{L,\rho} \subset \mathcal{D}_L$.

$$\mathcal{D}_L := \{d : \mathbb{R} \rightarrow \mathbb{R} \mid \mathcal{G}[d]_{L,\tau} \in \ell^1(\mathbb{Z}), \forall \tau \in [0, L)\} \quad (10a)$$

$$\mathcal{P}_{L,\rho} := \{d \in \mathcal{D}_L \mid \mathcal{F}[\mathcal{G}[d]_{L,\tau}](\Omega) = 0, \forall \tau \in [0, L), \forall \Omega \in (\rho L, \pi)\}. \quad (10b)$$

This definition is based on the quasiperiodicity in [Muramatsu \(2022\)](#). Let $\omega_0 := 2\pi/L$ and $n\omega_0$ be the fundamental and harmonic frequencies of the quasiperiodic disturbance, respectively.

The QDOB, which estimates and compensates for the quasiperiodic disturbance, is

$$\mathcal{L}[\hat{d}(t)] = Q(s)\mathcal{L}[\xi(t) - u(t)] \quad (11a)$$

$$\mathcal{L}[\xi(t)] = B(s)P_n^{-1}(s)\mathcal{L}[y(t)] \quad (11b)$$

$$u(t) = r(t) - \hat{d}(t), \quad (11c)$$

where $\hat{d}(t) \in \mathbb{R}$ is the estimated quasiperiodic disturbance. The QDOB is composed of a first-order low-pass filter

$$B(s) := \frac{\omega_b}{s + \omega_b} \quad (12)$$

and the Q-filter

$$Q(s) := \frac{\omega_c L(1 + \Phi(s))}{(\omega_c L + 2) + (\omega_c L - 2)\Phi(s)} \quad (13a)$$

$$\omega_c := \frac{2}{L} \tan\left(\frac{L}{2}\rho\right), \quad (13b)$$

using the linear-phase low-pass filter $\Phi(s)$:

$$\Phi(s) := e^{-\kappa Ts} \prod_{i=1}^l \varphi_i(s) \quad (14a)$$

$$\varphi_i(s) := \frac{1}{\gamma_i} \sum_{n=-N}^N \alpha_i(n) e^{(n-N)T\bar{U}_i s} \quad (14b)$$

$$\alpha_i(n) := w(n, N)h(n, \omega_i, U_i) \quad (14c)$$

$$w(n, N) := \begin{cases} 0.42 + 0.5 \cos(n\pi/N) \\ +0.08 \cos(2n\pi/N) & \text{if } |n| \leq N \\ 0 & \text{if } |n| > N, \end{cases} \quad (14d)$$

$$h(n, \omega_i, U_i) := \begin{cases} U_i \omega_i / \pi & \text{if } n = 0 \\ \sin(n U_i \omega_i) / (n \pi) & \text{if } n \neq 0 \end{cases} \quad (14e)$$

$$\gamma_i := \max_{\Omega \in [0, \pi]} \left| \alpha_i(0) + 2 \sum_{n=1}^N \alpha_i(n) \cos(n \Omega) \right| \quad (14f)$$

$$U_i := \begin{cases} T & \text{if } i = 1 \\ \pi / \omega_{i-1} & \text{otherwise} \end{cases} \quad (14g)$$

$$\omega_i := \begin{cases} \omega_a & \text{if } i = l \\ 2c\pi / U_i & \text{otherwise,} \end{cases} \quad c = \frac{1}{2} \left(\frac{T \omega_a}{\pi} \right)^{1/l} \quad (14h)$$

$$N := \min\{\max(\mathcal{N}), N_{\max}\} \quad (14i)$$

$$\mathcal{N} := \{n \in \mathbb{Z}_{>0} \mid n \leq (L - T) / \sum_{i=1}^l U_i\}. \quad (14j)$$

The parameters $T \in \mathbb{R}_{>0}$, $\omega_a \in \mathbb{R}_{>0}$, $l \in \mathbb{Z}_{>0}$, and $N_{\max} \in \mathbb{Z}_{>0}$ denote the sampling time, cutoff frequency, number of stages, and maximum order, respectively. This linear-phase low-pass filter can be equivalently expressed as (4). The Q-filter is based on the periodic/apperiodic separation filter (Muramatsu (2022); Muramatsu and Katsura (2019)) whose time delays are multiplied by zero-phase low-pass filters. Consequently, the open-loop transfer function $\Gamma(s)$ of the QDOB is

$$\Gamma(s) = \frac{\omega_c L}{2} \frac{1 + \Phi(s)}{1 - \Phi(s)} \frac{\omega_b}{s + \omega_b}, \quad (3)$$

and its sensitivity and complementary sensitivity functions are

$$S(s) := \frac{1}{1 + \Gamma(s)}, \quad T(s) := \frac{\Gamma(s)}{1 + \Gamma(s)}, \quad (15)$$

respectively.

The QDOB is discretized by two methods. The Q-filter $Q(s)$ is discretized by $e^{-Ts} \rightarrow z^{-1}$, and the transfer function $B(s)P_n^{-1}(s)$ is discretized by the backward Euler method $s \rightarrow (1 - z^{-1})/T$. Then, the open-loop transfer function in the discrete-time representation is

$$\tilde{\Gamma}(z) = \frac{\omega_c L}{2} \frac{1 + \tilde{\Phi}(z)}{1 - \tilde{\Phi}(z)} \frac{\omega_b T z}{(1 + \omega_b T)z - 1}, \quad (16)$$

where

$$\tilde{\Phi}(z) := z^{-\kappa} \prod_{i=1}^l \tilde{\varphi}_i(z) \quad (17a)$$

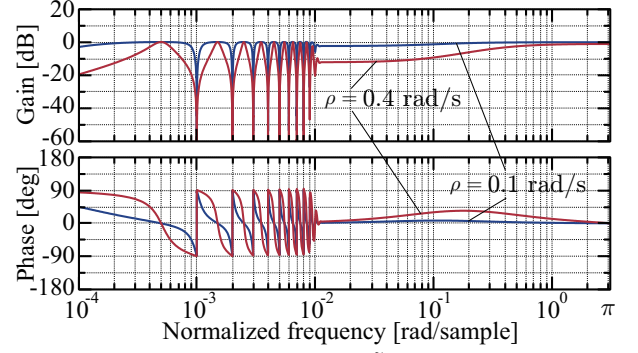
$$\tilde{\varphi}_i(z) := \frac{\sum_{n=-N}^N w(n, N) h(n, \omega_i, U_i) z^{(n-N)U_i}}{\sum_{n=-N}^N w(n, N) h(n, \omega_i, U_i)}. \quad (17b)$$

Accordingly, the sensitivity and complementary sensitivity functions in the discrete-time representation are

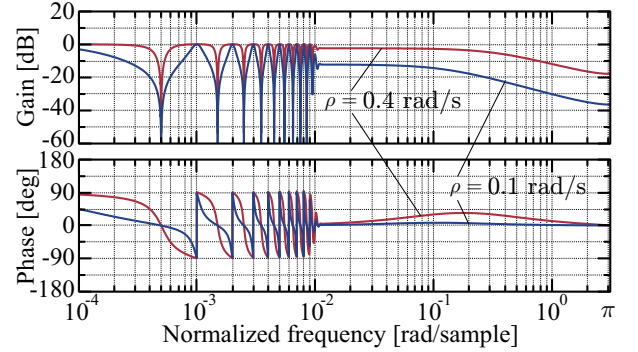
$$\tilde{S}(z) := \frac{1}{1 + \tilde{\Gamma}(z)}, \quad \tilde{T}(z) := \frac{\tilde{\Gamma}(z)}{1 + \tilde{\Gamma}(z)}, \quad (18)$$

respectively. Fig. 1 shows the Bode plots of the sensitivity, complementary sensitivity, and open-loop transfer functions in the discrete-time representation. As shown in Fig. 1(a), the QDOB can expand the harmonic suppression bandwidth by increasing the separation frequency ρ without the waterbed effect. See Muramatsu (2025) for the detailed derivation, design, analyses, and discretization of the QDOB, including the Bode plots of the functions in the continuous-time representation.

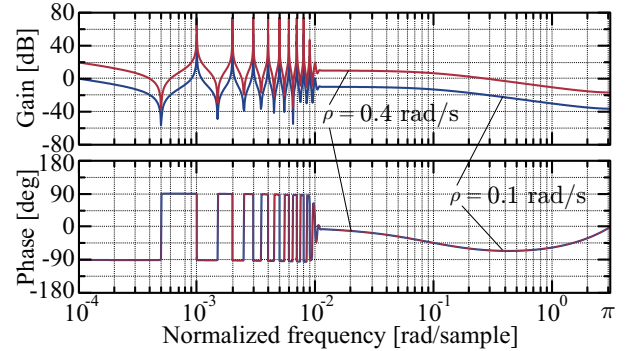
Remark 2.1 describes the modifications to Muramatsu (2025), and Remark 2.2 introduces how to design the QDOB on the basis of Muramatsu (2025).



(a) Sensitivity function $\tilde{S}(e^{j\Omega})$ in (18).



(b) Complementary sensitivity function $\tilde{T}(e^{j\Omega})$ in (18).



(c) Open-loop transfer function $\tilde{\Gamma}(e^{j\Omega})$ in (16).

Fig. 1. Bode plots of the QDOB in the discrete-time representation with $l = 3$, $N_{\max} = 256$, $\omega_0 = 1$ rad/s, $\omega_a = 10$ rad/s, $\omega_b = 100$ rad/s, and $T = 1$ ms.

Remark 2.1. The normalization $1/\gamma_i$ of (14b) for the linear-phase low-pass filter $\Phi(s)$ has been modified so that the gain of the filter satisfies $|\Phi(j\omega)| \leq 1$. In Muramatsu (2025), it was normalized by the DC gain $\gamma_i = \alpha_i(0) + 2 \sum_{n=1}^N \alpha_i(n)$ by neglecting passband ripple of the filter. Additionally, rounded $\bar{U}_i T$ and $\bar{L} T$ are used for the continuous-time representation instead of U_i and L in the time delays. Lastly, minor errors in the set $(\rho L, \pi]$ for Ω of (10b) in Definition 2.1 and of the upper limit of the summation of (14j) have been corrected.

Remark 2.2. The crucial hyperparameters of the QDOB for the sensitivity design are ω_a , ω_b , and ρ . The sensitivity function suppresses harmonics at frequencies below ω_a , and its gain can be less than 1 at frequencies below ω_b . Additionally, the gain of the complementary sensitivity function decreases for robust stability at frequencies above ω_b . The angular frequencies ω_a and ω_b are adjusted to design the sensitivity and complementary sensitivity func-

tions within the condition $\omega_a \ll \omega_b$, which maintains the phase of the open-loop transfer function within -90 deg. to 90 deg. at frequencies below the Nyquist frequency. The separation frequency $\rho \in [0, \pi/L]$ changes the harmonic suppression bandwidth such that $20 \log |S(j\omega)| < -3$ dB $\forall \omega \in [n\omega_0 - \rho, n\omega_0 + \rho] \cap [0, \omega_a]$ around the harmonic frequencies $n\omega_0$.

Based on the preliminaries, this paper discusses the waterbed effect on the sensitivity functions $S(s)$ and $\tilde{S}(z)$ in the continuous-time and discrete-time representations.

3. WATERBED EFFECT ON QDOB

3.1 Main Results

The main results of this paper are two theorems that apply a Bode-like sensitivity integral to the QDOB in the continuous-time or discrete-time representation. Two lemmas are provided for the proofs of the theorems.

Lemma 3.1. Suppose (14) and $g \in \mathbb{R}_{\geq 0}$; then,

$$\mathcal{S}_g := \{s \in \mathbb{C}_+ \mid \operatorname{Re}[s] > g\} \quad (19a)$$

$$|\Phi(s)| < \max_{\operatorname{Re}[s]=g} |\Phi(s)|, \quad \forall s \in \mathcal{S}_g. \quad (19b)$$

Proof. The proof is in Appendix A.

Lemma 3.2. The open-loop transfer function (3) has no poles in the open right-half plane.

Proof. The proof is in Appendix B.

Theorem 3.1. Suppose the open-loop transfer function (3). Then, the sensitivity function (15) in the continuous-time representation satisfies

$$\lim_{\varepsilon \rightarrow 0^+} \int_0^\infty \ln |S(\varepsilon + j\omega)| d\omega = -\frac{\pi\omega_b\omega_c L}{4}. \quad (20)$$

Proof. The proof is in Appendix C.

Theorem 3.2. Suppose the open-loop transfer function (16). Then, the sensitivity function (18) in the discrete-time representation satisfies

$$\begin{aligned} \lim_{\varepsilon \rightarrow 1^+} \int_0^{2\pi} \ln |\tilde{S}(\varepsilon e^{j\Omega})| d\Omega \\ = 2\pi \ln(2 + 2\omega_b T) - 2\pi \ln(2 + 2\omega_b T + \omega_b \omega_c L T). \end{aligned} \quad (21)$$

Proof. The proof is in Appendix D.

From the theorems, the Bode-like sensitivity integrals (20) and (21) decrease in both continuous-time and discrete-time representations as ω_b and/or ρ increases. This is consistent with Remark 2.2, the gain of the sensitivity function decreases as the parameters increase. Note that ω_c is determined by ρ according to (13b), and they are in a monotonic relationship. These suggest that the QDOB can extend the harmonic suppression bandwidth without a sensitivity tradeoff with the decrease in the integral. In contrast, ω_a does not affect the integrals. This implies that the band stops around the harmonic frequencies below ω_a are restricted by the sensitivity tradeoff. Fig. 2 illustrates the relationship among the gain of the sensitivity function, ω_a , ω_b , ω_c , and ρ . It shows that ω_b extends the suppression bandwidth horizontally, and $\omega_c L$ deepens the attenuation depth vertically. Meanwhile, there exists the waterbed

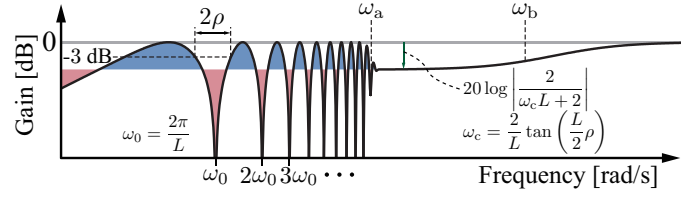


Fig. 2. Illustrative diagram for the gains of the sensitivity functions: $S(s)$ in (15) and $\tilde{S}(z)$ in (18) of the QDOB.

Table 1. Seven parameter settings and theoretical values of the Bode-like sensitivity integrals δ_{ct} and δ_{dt} in (22) with $T = 1$ ms.

	ω_0	ω_b	ρ	δ_{ct}	δ_{dt}
P ₁	1 rad/s	100 rad/s	0.1 rad/s	-51.0	-0.18
P ₂	1 rad/s	100 rad/s	0.25 rad/s	-157.1	-0.55
P ₃	10 rad/s	400 rad/s	1.476 rad/s	-314.2	-0.84
P ₄	1 rad/s	200 rad/s	0.25 rad/s	-314.2	-0.97
P ₅	1 rad/s	0.1 rad/s	0.25 rad/s	-0.16	-0.63×10^{-3}
P ₆	1 rad/s	0.5 rad/s	0.25 rad/s	-0.79	-3.14×10^{-3}
P ₇	1 rad/s	1 rad/s	0.25 rad/s	-1.57	-6.27×10^{-3}

effect with ω_a as the red region of the reduced gain and the blue region of the increased gain, while the gain does not exceed 0 dB.

Theorems 3.1 and 3.2 employ the Bode-like sensitivity integrals based on the limits avoiding the singularities on the imaginary axis and unit disk because the sensitivity function has an infinite and finite number of roots, respectively. Although the QDOB does not satisfy the assumptions of the existing Bode sensitivity integrals, the Bode-like sensitivity integrals (20) and (21) turn out to be consistent with the right-hand sides of the Bode sensitivity integrals (1) and (2), respectively.

3.2 Numerical Results

Numerical examples are provided to verify the convergence of the integrals: $\int_0^w \ln |S(j\omega)| d\omega$ and $\int_0^w \ln |\tilde{S}(e^{j\Omega})| d\Omega$ with respect to the upper limit of integration w toward (20) and (21). For the validation, parameter settings of Table 1 for the hyperparameters: ω_0 , ω_b , and ρ are considered. The theoretical values from (20) and (21) are expressed as

$$\delta_{ct} := -\frac{\pi\omega_b\omega_c L}{4} = -\frac{\pi\omega_b}{2} \tan\left(\frac{\pi\rho}{\omega_0}\right) \quad (22a)$$

$$\begin{aligned} \delta_{dt} &:= 2\pi \ln(2 + 2\omega_b T) - 2\pi \ln(2 + 2\omega_b T + \omega_b \omega_c L T) \\ &= 2\pi \ln(1 + \omega_b T) \\ &\quad - 2\pi \ln(1 + \omega_b T + \omega_b T \tan(\pi\rho/\omega_0)). \end{aligned} \quad (22b)$$

The numerical results are shown in Fig. 3. In the continuous-time cases of Fig. 3(a) and (c), the integral values asymptotically converge toward δ_{ct} as w increases. In the discrete-time cases of Fig. 3(b) and (d), the integral values reach δ_{dt} at $w = \pi$. Note that

$$\int_0^{2\pi} \ln |\tilde{S}(e^{j\Omega})| d\Omega = 2 \int_0^\pi \ln |\tilde{S}(e^{j\Omega})| d\Omega \quad (23)$$

based on $|\tilde{S}(e^{j\Omega})| = |\tilde{S}(e^{-j\Omega})|$ and $|\tilde{S}(e^{j\Omega})| = |\tilde{S}(e^{j(\Omega+2\pi)})|$.

Although Theorems 3.1 and 3.2 hold regardless of the relationship between ω_a and ω_b , the convergences of the integral values are different between $\omega_a \ll \omega_b$ [Fig. 3(a)

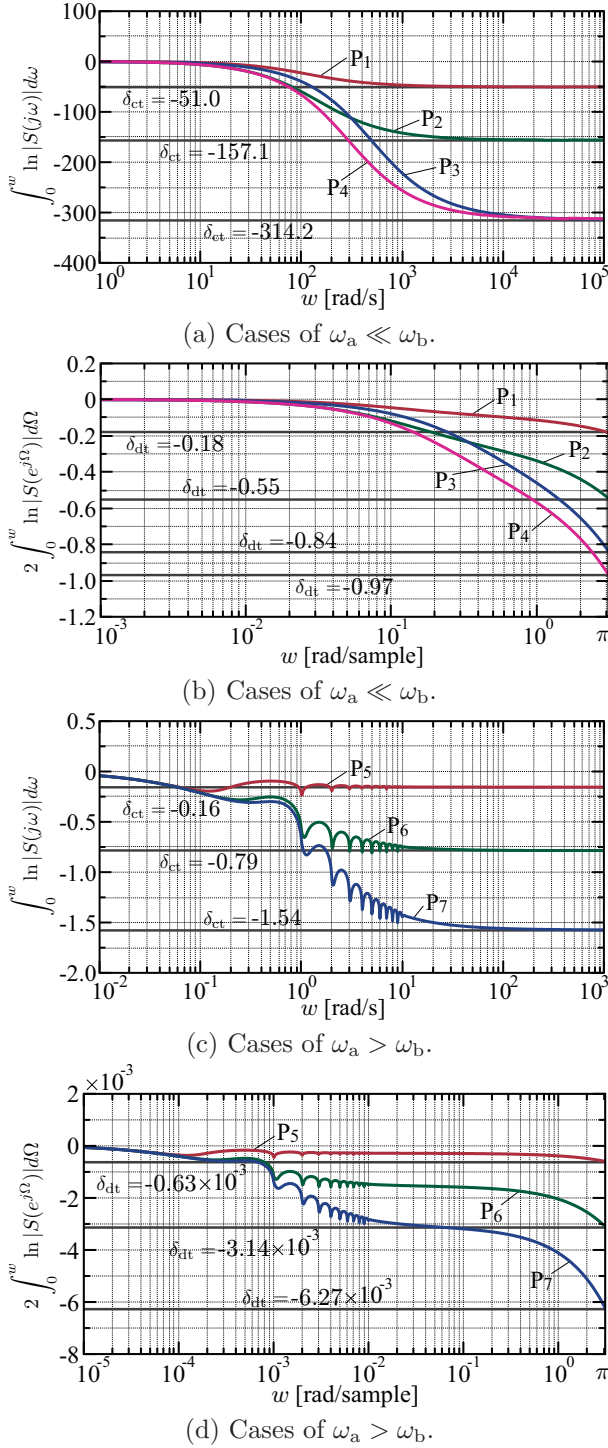


Fig. 3. Convergence of the numerical Bode-like sensitivity integrals toward the theoretical values δ_{ct} and δ_{dt} in (22) with $l = 3$, $N_{\max} = 256$, $\omega_a = 10$ rad/s, $T = 1$ ms, and Table 1.

and (b)] and $\omega_a > \omega_b$ [Fig. 3(c) and (d)]. If $\omega_a > \omega_b$, the gains $|S(j\omega)|$ and $|\tilde{S}(e^{j\Omega})|$ repeatedly increase and decrease while converging. These increases correspond to the amplification of aperiodic disturbances and can cause a shift in harmonic suppression frequencies, which usually happen with conventional repetitive control. Thus, the avoidance of the sensitivity tradeoff in Theorems 3.1 and 3.2 does not prevent local amplification of the gain.

To avoid the local amplification, the phase of the open-loop transfer function within ± 90 deg. is essential. To discuss this, this paper considers the following proposition.

Proposition 3.3. Suppose an open-loop transfer function $\Gamma(j\omega)$ and sensitivity function $S(j\omega) = (1 + \Gamma(j\omega))^{-1}$. Then, $|\angle\Gamma(j\omega)| \leq \pi/2 \Rightarrow |S(j\omega)| \leq 1$.

Proof. $|\angle\Gamma(j\omega)| \leq \pi/2 \Rightarrow \text{Re}[\Gamma(j\omega)] \geq 0 \Rightarrow (1 + \text{Re}[\Gamma(j\omega)])^2 + \text{Im}[\Gamma(j\omega)]^2 \geq 1 \Rightarrow |S(j\omega)| = ((1 + \text{Re}[\Gamma(j\omega)])^2 + \text{Im}[\Gamma(j\omega)]^2)^{-1/2} \leq 1$.

On the basis of Remark 2.2 and Proposition 3.3, the parameter design $\omega_a \ll \omega_b$, which makes the phase of the open-loop transfer function within ± 90 deg. at frequencies below the Nyquist frequency, prevents local amplification of the gain at the frequencies. Furthermore, the separation frequency ρ does not affect the phase of the open-loop transfer function $\Gamma(s)$, and the phase exists within ± 90 deg. regardless of ρ , as shown in Fig. 1(c). This indicates that the gain of the sensitivity function always satisfies $|S(j\omega)| \leq 1$ regardless of ρ if $\omega_a \ll \omega_b$. These results explain how the increase in the separation frequency ρ extends the harmonic suppression bandwidth while decreasing the Bode-like sensitivity integral, without causing amplification at other frequencies below the Nyquist frequency. For the continuous-time representation, at frequencies beyond the Nyquist frequency, the low-pass filter $B(j\omega)$ and sensitivity function $S(j\omega)$ asymptotically approach zero and one, respectively, as the frequency increases.

4. CONCLUSION

This paper examined the waterbed effect in the QDOB proposed by Muramatsu (2025), which estimates and compensates for the quasiperiodic disturbance of Definition 2.1. Compared to conventional periodic-disturbance-compensation control, the advantage of the QDOB is the simultaneous realization of the wideband harmonic suppression, non-amplification of aperiodic disturbances, and proper harmonic suppression frequencies.

In this paper, Theorems 3.1 and 3.2 indicated the avoided sensitivity tradeoff, where the extension of harmonic suppression bandwidth for the sensitivity function also reduces the Bode-like sensitivity integral. Moreover, the numerical results and Proposition 3.3 showed the waterbed effect on the QDOB, where the phase of the open-loop transfer function within ± 90 deg. results in the non-amplification of aperiodic disturbances and proper harmonic suppression frequencies. This clarified why the parameter condition $\omega_a \ll \omega_b$ in Remark 2.2 is necessary for the avoidance of the waterbed effect.

These results support the advantage of the QDOB and clarify its practical potential for improving automatic mechanical and electrical systems with quasiperiodic, periodic, or harmonic disturbances, such as friction or gravitational force with repetitive motion, wind disturbances, torque ripple, and current ripple. However, there remain two problems: how to find γ_i defined in (14f) for implementation, and the waterbed effect associated with discretization methods.

Appendix A. PROOF OF LEMMA 3.1

The linear-phase low-pass filter $\Phi(s)$ in (14) is analytic and can be expressed as (4). Let

$$\mathcal{E}_g := \{\xi \in \mathbb{C} \mid |\xi| < e^{-Tg}\}, \quad \xi := e^{-Ts} \quad (\text{A.1a})$$

$$H(\xi) := \prod_{i=1}^l \sum_{n=-N}^N \frac{\alpha_i(n)}{\gamma_i} \xi^{(N-n)\bar{U}_i}. \quad (\text{A.1b})$$

Based on (4),

$$\xi \in \mathcal{E}_g \Leftrightarrow s \in \mathcal{S}_g, \quad |\xi| = e^{-Tg} \Leftrightarrow \text{Re}[s] = g \quad (\text{A.2a})$$

$$\Phi(s) = e^{-\kappa Ts} H(e^{-Ts}). \quad (\text{A.2b})$$

Since $H(\xi)$ is nonconstant and analytic in the open disk \mathcal{E}_g and continuous on the closure of \mathcal{E}_g , the maximum modulus principle gives

$$|H(\xi)| < \max_{|\xi|=e^{-Tg}} |H(\xi)|, \quad \forall \xi \in \mathcal{E}_g. \quad (\text{A.3})$$

By the change of variable $\xi = e^{-Ts}$,

$$|H(e^{-Ts})| = |e^{\kappa Ts}| |\Phi(s)| = e^{\kappa T \text{Re}[s]} |\Phi(s)| \quad (\text{A.4a})$$

$$\begin{aligned} \max_{|\xi|=e^{-Tg}} |H(\xi)| &= \max_{\text{Re}[s]=g} |H(e^{-Ts})| \\ &= \max_{\text{Re}[s]=g} |e^{\kappa Ts} \Phi(s)| = e^{\kappa Tg} \max_{\text{Re}[s]=g} |\Phi(s)|. \end{aligned} \quad (\text{A.4b})$$

Hence,

$$e^{\kappa T \text{Re}[s]} |\Phi(s)| < e^{\kappa Tg} \max_{\text{Re}[s]=g} |\Phi(s)|, \quad \forall s \in \mathcal{S}_g. \quad (\text{A.5})$$

Because $e^{\kappa T \text{Re}[s]} > e^{\kappa Tg} \geq 1$, $\forall s \in \mathcal{S}_g$, we have

$$|\Phi(s)| < \max_{\text{Re}[s]=g} |\Phi(s)|, \quad \forall s \in \mathcal{S}_g. \quad (\text{A.6})$$

Appendix B. PROOF OF LEMMA 3.2

The poles of (3) are roots of $s + \omega_b$ and $1 - \Phi(s)$. The root of $s + \omega_b$ is $s = -\omega_b$ in the open left-half plane. The linear-phase low-pass filter $\Phi(s)$ in (14) consists of multiple linear-phase low-pass filters $\varphi_i(s)$ in (14b). Its gain is

$$\begin{aligned} |\varphi_i(j\omega)| &= \frac{1}{\gamma_i} \left| \alpha_i(0) + \sum_{n=1}^N \alpha_i(n) (e^{jnT\bar{U}_i\omega} + e^{-jnT\bar{U}_i\omega}) \right| \\ &= \frac{1}{\gamma_i} \left| \alpha_i(0) + 2 \sum_{n=1}^N \alpha_i(n) \cos(nT\bar{U}_i\omega) \right| \end{aligned} \quad (\text{B.1})$$

using the property $\alpha_i(n) = \alpha_i(-n)$ of even functions. Eqs. (14b) and (14f) yield $|\varphi_i(j\omega)| \leq 1$, $\forall \omega \in \mathbb{R}$, and

$$|\Phi(j\omega)| = \prod_{i=1}^l |\varphi_i(j\omega)| \leq 1, \quad \forall \omega \in \mathbb{R}. \quad (\text{B.2})$$

Lemma 3.1 gives

$$|\Phi(s)| < \max_{\text{Re}[s]=0} |\Phi(s)|, \quad \forall s \in \mathcal{S}_0 = \mathbb{C}_+. \quad (\text{B.3})$$

These yield

$$|\Phi(s)| < \max_{\omega \in \mathbb{R}} |\Phi(j\omega)| \leq 1, \quad \forall s \in \mathbb{C}_+, \quad (\text{B.4})$$

which implies $\Phi(s) \neq 1$, $\forall s \in \mathbb{C}_+$, and $1 - \Phi(s)$ has no roots in \mathbb{C}_+ . Therefore, the open-loop transfer function (3) has no poles in the open right-half plane.

Appendix C. PROOF OF THEOREM 3.1

Let a simply connected region $\mathcal{C}_\varepsilon \subset \mathbb{C}_+$ and simple closed contour $\mathcal{D}_{\varepsilon,\delta} \subset \mathcal{C}_\varepsilon$ be

$$\mathcal{C}_\varepsilon := \{s \in \mathbb{C} \mid \text{Re}[s] > \varepsilon\}, \quad \varepsilon \in (0, 1/2) \quad (\text{C.1a})$$

$$\mathcal{D}_{\varepsilon,\delta} := \{\delta + jr \mid -R_{\varepsilon,\delta} \leq r \leq R_{\varepsilon,\delta}\} \cup \mathcal{A}_{\varepsilon,\delta} \quad (\text{C.1b})$$

$$\mathcal{A}_{\varepsilon,\delta} := \{\delta + R_{\varepsilon,\delta} e^{j\theta} \mid \theta \in \Theta\} \quad (\text{C.1c})$$

$$\Theta := (-\pi/2, \pi/2), \quad R_{\varepsilon,\delta} := 2\omega_b\omega_c L\phi_\varepsilon / (\delta - \varepsilon) \quad (\text{C.1d})$$

$$\phi_\varepsilon := 1 / (1 - \max_{\text{Re}[s]=\varepsilon} |\Phi(s)|) \in [1, \infty) \quad (\text{C.1e})$$

$$\delta \in \Delta_\varepsilon := \{\delta \in (\varepsilon, 1/2) \mid R_{\varepsilon,\delta} > 2(\delta + \omega_b)\} \quad (\text{C.1f})$$

using the linear-phase low-pass filter $\Phi(s)$ in (14a). On the region $\mathcal{A}_{\varepsilon,\delta} \subset \mathcal{S}_\delta$, the non-constant filter $\Phi(s)$ satisfies

$$|\Phi(s)| < \max_{\text{Re}[s]=\delta} |\Phi(s)| < \max_{\text{Re}[s]=\varepsilon} |\Phi(s)| < 1 \quad (\text{C.2a})$$

$$1 / (1 - |\Phi(s)|) < \phi_\varepsilon < \infty \quad (\text{C.2b})$$

based on Lemma 3.1. Given ε , ϕ_ε is a finite constant independent of δ . Using the following relationships

$$\left| \frac{1 + \Phi(s)}{1 - \Phi(s)} \right| \leq 2\phi_\varepsilon, \quad \forall s \in \mathcal{A}_{\varepsilon,\delta}. \quad (\text{C.3a})$$

$$\begin{aligned} R_{\varepsilon,\delta} > 2(\delta + \omega_b) &\Rightarrow -(\delta + \omega_b) > -R_{\varepsilon,\delta}/2 \\ &\Rightarrow 1 / (R_{\varepsilon,\delta} - \delta - \omega_b) < 2 / R_{\varepsilon,\delta}, \end{aligned} \quad (\text{C.3b})$$

the open-loop transfer function (3) is bounded as

$$\begin{aligned} \sup_{s \in \mathcal{A}_{\varepsilon,\delta}} |\Gamma(s)| &\leq \frac{\omega_b\omega_c L\phi_\varepsilon}{R_{\varepsilon,\delta} - \delta - \omega_b} < \frac{2\omega_b\omega_c L\phi_\varepsilon}{R_{\varepsilon,\delta}} = \delta - \varepsilon \\ &< 1/2. \end{aligned} \quad (\text{C.4})$$

Hence,

$$\log(1 + \Gamma(s)) = \Gamma(s) + \sum_{n=2}^{\infty} (-1)^{n+1} \frac{\Gamma(s)^n}{n} \quad (\text{C.5})$$

$$\begin{aligned} |\log(1 + \Gamma(s)) - \Gamma(s)| &\leq \sum_{n=0}^{\infty} |\Gamma(s)|^n - 1 - |\Gamma(s)| \\ &\leq \frac{|\Gamma(s)|^2}{1 - |\Gamma(s)|} < 2|\Gamma(s)|^2. \end{aligned} \quad (\text{C.6})$$

These and the estimation lemma give

$$\left| \int_{\mathcal{A}_{\varepsilon,\delta}} \log(1 + \Gamma(s)) - \Gamma(s) ds \right| < 2\pi R_{\varepsilon,\delta} \sup_{s \in \mathcal{A}_{\varepsilon,\delta}} |\Gamma(s)|^2 \quad (\text{C.7})$$

with the length $\pi R_{\varepsilon,\delta}$ of $\mathcal{A}_{\varepsilon,\delta}$. The limit of the upper bound equals zero as

$$\begin{aligned} \lim_{\delta \rightarrow \varepsilon^+} R_{\varepsilon,\delta} \sup_{s \in \mathcal{A}_{\varepsilon,\delta}} |\Gamma(s)|^2 &\leq \lim_{\delta \rightarrow \varepsilon^+} R_{\varepsilon,\delta} \left(\frac{2\omega_b\omega_c L\phi_\varepsilon}{R_{\varepsilon,\delta}} \right)^2 \\ &\leq \lim_{\delta \rightarrow \varepsilon^+} 2\omega_b\omega_c L\phi_\varepsilon (\delta - \varepsilon) = 0. \end{aligned} \quad (\text{C.8})$$

Thus, $\lim_{\delta \rightarrow \varepsilon^+} \left| \int_{\mathcal{A}_{\varepsilon,\delta}} \log(1 + \Gamma(s)) - \Gamma(s) ds \right| = 0$, and

$$\lim_{\delta \rightarrow \varepsilon^+} \int_{\mathcal{A}_{\varepsilon,\delta}} \log(1 + \Gamma(s)) ds = \lim_{\delta \rightarrow \varepsilon^+} \int_{\mathcal{A}_{\varepsilon,\delta}} \Gamma(s) ds. \quad (\text{C.9})$$

In \mathbb{C}_+ , the sensitivity function $S(s) = 1 / (1 + \Gamma(s))$ has no zeros owing to Lemma 3.2 and no poles because the QDOB is stable according to Muramatsu (2025) with (B.4). Hence, $S(s)$ is analytic in \mathbb{C}_+ . For the analytic function $S(s)$ that has no zeros in the simply connected region \mathcal{C}_ε , there exists a single-valued analytic branch of the logarithm of $S(s)$ in $\mathcal{D}_{\varepsilon,\delta}$ according to Ahlfors (1979). Let $\log(S(s))$ denote this single-valued analytic branch such that $\log(S(s)) = \ln|S(s)| + j\angle S(s)$. We apply the Cauchy integral theorem to the branch $\log(S(s))$ on $\mathcal{D}_{\varepsilon,\delta}$ traversed counterclockwise:

$$\oint_{\mathcal{D}_{\varepsilon,\delta}} \log(S(s)) ds = 0. \quad (\text{C.10})$$

Then, (C.10) can be transformed as follows

$$\int_{\delta+jR_{\varepsilon,\delta}}^{\delta-jR_{\varepsilon,\delta}} \log(S(s))ds + \int_{\mathcal{A}_{\varepsilon,\delta}} \log(S(s))ds = 0 \quad (\text{C.11a})$$

$$j \int_{-R_{\varepsilon,\delta}}^{R_{\varepsilon,\delta}} \log(S(\delta + j\omega))d\omega = \int_{\mathcal{A}_{\varepsilon,\delta}} \log(S(s))ds \quad (\text{C.11b})$$

$$\int_{-R_{\varepsilon,\delta}}^{R_{\varepsilon,\delta}} \ln |S(\delta + j\omega)|d\omega = \text{Im} \left[\int_{\mathcal{A}_{\varepsilon,\delta}} \log(S(s))ds \right]. \quad (\text{C.11c})$$

The Bode-like sensitivity integral is calculated as

$$\begin{aligned} \lim_{\varepsilon \rightarrow 0^+} \int_0^{\infty} \ln |S(\varepsilon + j\omega)|d\omega &= \lim_{\delta \rightarrow 0^+} \frac{1}{2} \int_{-\infty}^{\infty} \ln |S(\delta + j\omega)|d\omega \\ &= \frac{1}{2} \lim_{\varepsilon \rightarrow 0^+} \lim_{\delta \rightarrow \varepsilon^+} \int_{-R_{\varepsilon,\delta}}^{R_{\varepsilon,\delta}} \ln |S(\delta + j\omega)|d\omega \\ &= \frac{1}{2} \lim_{\varepsilon \rightarrow 0^+} \lim_{\delta \rightarrow \varepsilon^+} \text{Im} \left[\int_{\mathcal{A}_{\varepsilon,\delta}} \log(S(s))ds \right] \\ &= -\frac{1}{2} \lim_{\varepsilon \rightarrow 0^+} \lim_{\delta \rightarrow \varepsilon^+} \text{Im} \left[\int_{\mathcal{A}_{\varepsilon,\delta}} \log(1 + \Gamma(s))ds \right]. \end{aligned} \quad (\text{C.12})$$

From (C.9),

$$\begin{aligned} \lim_{\delta \rightarrow \varepsilon^+} \int_{\mathcal{A}_{\varepsilon,\delta}} \log(1 + \Gamma(s))ds &= \lim_{\delta \rightarrow \varepsilon^+} \int_{\mathcal{A}_{\varepsilon,\delta}} \Gamma(s)ds \\ &= j \lim_{\delta \rightarrow \varepsilon^+} \int_{-\pi/2}^{\pi/2} \Gamma(\delta + R_{\varepsilon,\delta}e^{j\theta})R_{\varepsilon,\delta}e^{j\theta}d\theta. \end{aligned} \quad (\text{C.13})$$

The limit and integral can be interchanged on the basis of the dominated convergence theorem as

$$\begin{aligned} \lim_{\delta \rightarrow \varepsilon^+} \int_{-\pi/2}^{\pi/2} \Gamma(\delta + R_{\varepsilon,\delta}e^{j\theta})R_{\varepsilon,\delta}e^{j\theta}d\theta \\ &= \int_{-\pi/2}^{\pi/2} \lim_{\delta \rightarrow \varepsilon^+} \Gamma(\delta + R_{\varepsilon,\delta}e^{j\theta})R_{\varepsilon,\delta}e^{j\theta}d\theta \\ &= \frac{\omega_b\omega_c L}{2} \int_{-\pi/2}^{\pi/2} d\theta = \frac{\omega_b\omega_c L\pi}{2}, \end{aligned} \quad (\text{C.14})$$

which is based on

$$\lim_{\delta \rightarrow \varepsilon^+} R_{\varepsilon,\delta} = \infty \quad (\text{C.15a})$$

$$\begin{aligned} \lim_{\delta \rightarrow \varepsilon^+} |\Phi(\delta + R_{\varepsilon,\delta}e^{j\theta})| \\ \leq \lim_{\delta \rightarrow \varepsilon^+} \prod_{i=1}^l \sum_{n=-N}^N \left| \frac{\alpha_i(n)}{\gamma_i} \right| e^{((n-N)\bar{U}_i - \kappa)TR_{\varepsilon,\delta} \cos(\theta)} \\ = 0 \end{aligned} \quad (\text{C.15b})$$

$$\lim_{\delta \rightarrow \varepsilon^+} \Phi(\delta + R_{\varepsilon,\delta}e^{j\theta}) = 0, \quad \forall \theta \in \Theta \quad (\text{C.15c})$$

$$\begin{aligned} \lim_{\delta \rightarrow \varepsilon^+} \Gamma(\delta + R_{\varepsilon,\delta}e^{j\theta})R_{\varepsilon,\delta}e^{j\theta} \\ = \lim_{\delta \rightarrow \varepsilon^+} \frac{\omega_b\omega_c L}{2} \frac{1 + \Phi(\delta + R_{\varepsilon,\delta}e^{j\theta})}{1 - \Phi(\delta + R_{\varepsilon,\delta}e^{j\theta})} \frac{R_{\varepsilon,\delta}e^{j\theta}}{\delta + R_{\varepsilon,\delta}e^{j\theta} + \omega_b} \\ = \omega_b\omega_c L/2, \end{aligned} \quad (\text{C.15d})$$

and

$$|\Gamma(\delta + R_{\varepsilon,\delta}e^{j\theta})R_{\varepsilon,\delta}e^{j\theta}| \leq 2\omega_b\omega_c L\phi_\varepsilon, \quad (\text{C.16})$$

where this upper bound is an integrable function independent of δ .

From (C.12), (C.13), and (C.14), the Bode-like sensitivity integral for the QDOB is obtained as

$$\lim_{\varepsilon \rightarrow 0^+} \int_0^{\infty} \ln |S(\varepsilon + j\omega)|d\omega = -\frac{\omega_b\omega_c L\pi}{4}. \quad (\text{C.17})$$

Appendix D. PROOF OF THEOREM 3.2

Let a simply connected region $\mathcal{C}_\varepsilon \subset \mathbb{C}$ be

$$\mathcal{C}_\varepsilon = \{\tilde{z} \in \mathbb{C} \mid |\tilde{z}| < \varepsilon^{-1} < 1\}, \quad \tilde{z} := z^{-1}. \quad (\text{D.1})$$

Suppose the linear-phase low-pass filter $\tilde{\Phi}(z)$ in (17), open-loop transfer function $\tilde{\Gamma}(z)$ in (16), and sensitivity function $\tilde{S}(z)$. We substitute $z = \tilde{z}^{-1}$ for the functions, as follows

$$\hat{\Phi}(\tilde{z}) := \tilde{\Phi}(\tilde{z}^{-1}) = p_1\tilde{z} + p_2\tilde{z}^2 + \dots + p_L\tilde{z}^L \quad (\text{D.2a})$$

$$\hat{\Gamma}(\tilde{z}) := \tilde{\Gamma}(\tilde{z}^{-1}) = \frac{\omega_c L}{2} \frac{1 + \hat{\Phi}(\tilde{z})}{1 - \hat{\Phi}(\tilde{z})} \frac{\omega_b T}{1 + \omega_b T - \tilde{z}} \quad (\text{D.2b})$$

$$\hat{S}(\tilde{z}) := \tilde{S}(\tilde{z}^{-1}) = 1/(1 + \hat{\Gamma}(\tilde{z})), \quad (\text{D.2c})$$

where $p_1, p_2, \dots \in \mathbb{R}$. According to Ahlfors (1979), for the analytic function $\hat{S}(\tilde{z})$ that has no zeros in the simply connected region \mathcal{C}_ε , there exists a single-valued analytic branch of the logarithm of $\hat{S}(\tilde{z})$ in \mathcal{C}_ε . Let $\log(\hat{S}(\tilde{z}))$ denote this single-valued analytic branch such that $\log(\hat{S}(\tilde{z})) = \ln |\hat{S}(\tilde{z})| + j\angle \hat{S}(\tilde{z})$. In the open disk \mathcal{C}_ε , the analytic branch $\log(\hat{S}(\tilde{z}))$ has the following Maclaurin series

$$\log(\hat{S}(\tilde{z})) = \log(\hat{S}(0)) + a_1\tilde{z} + a_2\tilde{z}^2 + \dots \quad (\text{D.3})$$

with $a_1, a_2, \dots \in \mathbb{C}$. Accordingly,

$$\log(\tilde{S}(z)) = \log(\hat{S}(0)) + a_1z^{-1} + a_2z^{-2} + \dots \quad (\text{D.4})$$

Using this series, the contour integral of $\log(\tilde{S}(z))z^{-1}$ along $|z| = \varepsilon$ is

$$\begin{aligned} \lim_{\varepsilon \rightarrow 1^+} \oint_{|z|=\varepsilon} \log(\tilde{S}(z))z^{-1}dz \\ &= \lim_{\varepsilon \rightarrow 1^+} \oint_{|z|=\varepsilon} \log(\hat{S}(0))z^{-1} + a_1z^{-2} + \dots dz \\ &= j \lim_{\varepsilon \rightarrow 1^+} \int_0^{2\pi} \log(\hat{S}(0)) + a_1\varepsilon^{-1}e^{-j\Omega} + \dots d\Omega \\ &= j2\pi \log(\hat{S}(0)). \end{aligned} \quad (\text{D.5})$$

Meanwhile, the contour integral becomes

$$\begin{aligned} \lim_{\varepsilon \rightarrow 1^+} \oint_{|z|=\varepsilon} \log(\tilde{S}(z))z^{-1}dz \\ = \lim_{\varepsilon \rightarrow 1^+} \int_0^{2\pi} j \ln |\tilde{S}(\varepsilon e^{j\Omega})| - \angle \tilde{S}(\varepsilon e^{j\Omega}) d\Omega. \end{aligned} \quad (\text{D.6})$$

From the imaginary parts of (D.5) and (D.6), the Bode-like sensitivity integral for the discrete-time representation is

$$\begin{aligned} \lim_{\varepsilon \rightarrow 1^+} \int_0^{2\pi} \ln |\tilde{S}(\varepsilon e^{j\Omega})|d\Omega &= 2\pi \text{Re}[\log(\hat{S}(0))] \\ &= 2\pi \ln(2 + 2\omega_b T) - 2\pi \ln(2 + 2\omega_b T + \omega_b\omega_c LT). \end{aligned} \quad (\text{D.7})$$

REFERENCES

- Ahlfors, L.V. (1979). *Complex analysis*, volume 3. McGraw-Hill New York.
- Bode, H. (1945). *Network Analysis and Feedback Amplifier Design*. Bell Telephone Laboratories series. D. Van Nostrand Company.
- Bristow, D.A., Tharayil, M., and Alleyne, A.G. (2006). A survey of iterative learning control. *IEEE Control Systems Magazine*, 26(3), 96–114.

- Chang, W., Ariaei, F., and Jonckheere, E. (2023). Bode integral limitation for irrational systems. *IFAC-PapersOnLine*, 56(2), 4331–4336. doi:<https://doi.org/10.1016/j.ifacol.2023.10.1804>. 22nd IFAC World Congress.
- Chen, X. and Tomizuka, M. (2014). New repetitive control with improved steady-state performance and accelerated transient. *IEEE Transactions on Control Systems Technology*, 22(2), 664–675.
- Costa-Castelló, R. and Dormido, S. (2015). An interactive tool to introduce the waterbed effect. *IFAC-PapersOnLine*, 48(29), 259–264. doi:<https://doi.org/10.1016/j.ifacol.2015.11.246>.
- Ding, Y., Peng, H., Ma, J., Hara, S., and Chen, J. (2022). Bode integral: A unifier of control-relevant integral relations. *IFAC-PapersOnLine*, 55(25), 97–102. doi:<https://doi.org/10.1016/j.ifacol.2022.09.330>. 10th IFAC Symposium on Robust Control Design ROCOND 2022.
- Emami-Naeini, A. and de Roover, D. (2019). Bode's sensitivity integral constraints: The waterbed effect in discrete time. doi:<https://arxiv.org/abs/1903.01225>.
- Freudenberg, J. and Looze, D. (1985). Right half plane poles and zeros and design tradeoffs in feedback systems. *IEEE Transactions on Automatic Control*, 30(6), 555–565. doi:<https://doi.org/10.1109/TAC.1985.1104004>.
- Freudenberg, J. and Looze, D. (1987). A sensitivity tradeoff for plants with time delay. *IEEE Transactions on Automatic Control*, 32(2), 99–104. doi:<https://doi.org/10.1109/TAC.1987.1104547>.
- Gomez, G. and Goodwin, G. (1998). Generalization of integral constraints on sensitivity to time-delay systems. *IEEE Transactions on Automatic Control*, 43(7), 1008–1012. doi:<https://doi.org/10.1109/9.701114>.
- Hara, S., Yamamoto, Y., Omata, T., and Nakano, M. (1988). Repetitive control system: a new type servo system for periodic exogenous signals. *IEEE Transactions on Automatic Control*, 33(7), 659–668.
- Lai, J., Yin, X., Yin, X., and Jiang, L. (2021). Fractional order harmonic disturbance observer control for three-phase LCL-type inverter. *Control Engineering Practice*, 107, 104697. doi:<https://doi.org/10.1016/j.conengprac.2020.104697>.
- Li, L., Huang, W.W., Wang, X., Chen, Y.L., and Zhu, L. (2023). Periodic-disturbance observer using spectrum-selection filtering scheme for cross-coupling suppression in atomic force microscopy. *IEEE Transactions on Automation Science and Engineering*, 20(3), 2037–2048. doi:[10.1109/TASE.2022.3193116](https://doi.org/10.1109/TASE.2022.3193116).
- Mohtadi, C. (1990). Bode's integral theorem for discrete-time systems. *IEE Proceedings D (Control Theory and Applications)*, 137(2), 57–66.
- Muramatsu, H. and Katsura, S. (2018). An adaptive periodic-disturbance observer for periodic-disturbance suppression. *IEEE Transactions on Industrial Informatics*, 14(10), 4446–4456. doi:<https://doi.org/10.1109/TII.2018.2804338>.
- Muramatsu, H. and Katsura, S. (2019). Separated periodic/aperiodic state feedback control using periodic/aperiodic separation filter based on lifting. *Automatica*, 101, 458–466.
- Muramatsu, H. (2022). Separation and estimation of periodic/aperiodic state. *Automatica*, 140, 110263.
- Muramatsu, H. (2025). Quasiperiodic disturbance observer for wideband harmonic suppression. *IEEE Transactions on Control Systems Technology*, 33(5), 1895–1904. doi:<https://doi.org/10.1109/TCST.2025.3566560>.
- Nagarsheth, S.H. and Sharma, S.N. (2021). Some new rearrangements in sensitivity integrals and concerning inequalities with their application in control. *Results in Control and Optimization*, 4, 100036. doi:<https://doi.org/10.1016/j.rico.2021.100036>.
- Nie, K., Xue, W., Zhang, C., and Mao, Y. (2021). Disturbance observer-based repetitive control with application to optoelectronic precision positioning system. *J. Franklin Inst.*, 358(16), 8443–8469. doi:<https://doi.org/10.1016/j.jfranklin.2021.08.042>.
- Pipeleers, G., Demeulenaere, B., De Schutter, J., and Swevers, J. (2008). Robust high-order repetitive control: Optimal performance trade-offs. *Automatica*, 44(10), 2628–2634. doi:<https://doi.org/10.1016/j.automatica.2008.02.028>.
- Sariyildiz, E. and Ohnishi, K. (2013a). Design constraints of disturbance observer in the presence of time delay. In *Proceedings of the IEEE International Conference on Mechatronics*, 69–74. doi:<https://doi.org/10.1109/ICMECH.2013.6518513>.
- Sariyildiz, E. and Ohnishi, K. (2013b). Performance and robustness trade-off in disturbance observer design. In *Proceedings of the Annual Conference of IEEE Industrial Electronics Society*, 3681–3686. doi:<https://doi.org/10.1109/IECON.2013.6699721>.
- Skogestad, S. and Postlethwaite, I. (2005). *Multivariable feedback control: analysis and design*. John Wiley & sons.
- Songchon, T. and Longman, R. (2000). Iterative learning control and the waterbed effect. In *Astrodynamics Specialist Conference*, 4356.
- Sung, H.K. and Hara, S. (1988). Properties of sensitivity and complementary sensitivity functions in single-input single-output digital control systems. *International Journal of Control*, 48(6), 2429–2439. doi:<https://doi.org/10.1080/00207178808906338>.
- Tanaka, H. and Muramatsu, H. (2023). Infinite-impulse-response periodic-disturbance observer for harmonics elimination with wide band-stop bandwidths. *Mechanical Engineering Journal*, 10(2), 22–00362. doi:<https://doi.org/10.1299/mej.22-00362>.
- Wang, Y., Gao, F., and Doyle, F.J. (2009). Survey on iterative learning control, repetitive control, and run-to-run control. *Journal of Process Control*, 19(10), 1589–1600.
- Wu, B.F. and Jonckheere, E.A. (1992). A simplified approach to bode's theorem for continuous-time and discrete-time systems. *IEEE Transactions on Automatic Control*, 37(11), 1797–1802. doi:<https://doi.org/10.1109/9.173154>.
- Yang, Y., Cui, Y., Qiao, J., and Zhu, Y. (2023). Adaptive periodic-disturbance observer based composite control for sgcmg gimbal servo system with rotor vibration. *Control Engineering Practice*, 132, 105407. doi:<https://doi.org/10.1016/j.conengprac.2022.105407>.